Pure Appl. Chem., Vol. 83, No. 9, pp. 1721–1729, 2011.
doi:10.1351/PAC-CON-10-12-01

A series of tetranuclear [2 × 2] grid complexes derived from an asymmetric ligand: Structural differences based on metal ion affinities*

Takuya Shiga, Mao Noguchi, Takuto Matsumoto, Hiroki Sato, Hirotaka Tahira, Graham N. Newton, and Hiroki Oshio‡

Graduate School of Pure and Applied Sciences, University of Tsukuba, Tennodai 1-1-1, Tsukuba 305-8571, Japan

Abstract: A series of tetranuclear grid-type complexes were prepared by the reaction of the asymmetric multidentate ligand HL (HL = 2-[3-(2-hydroxyphenyl)-1*H*-pyrazol-5-yl]-6-pyridine carboxylic acid ethylester) with different metal sources. The tetranuclear copper complex, $[Cu_4(L1)_4(NO_3)_4(H_2O)_4]\cdot Et_2O\cdot 2MeOH$ (**1**, HL1 = 2-[3-(2-hydroxyphenyl)-1*H*-pyrazol-5-yl]-6-pyridine carboxylic acid methyl ester) consists of four ligands, four copper ions, four nitrate ions and four water molecules, forming a [2 × 2] grid structure, in which all four copper ions have the same coordination environment. On the other hand, the corresponding nickel and cobalt complexes, $[M_4(L2)_4(H_2O)_4]\cdot 4MeOH\cdot 6H_2O$ (M = Ni (**2**) and Co (**3**), (H_2L2 = 6-[1,3-dioxo-3-(2-phenyl)propionyl]pyridine-2-carboxylic acid)), have a similar grid core structure to the copper complex with four metal ions, four ligand molecules, and four water molecules, however, in these clusters there are two kinds of coordination site for the metal ions. Temperature-dependent magnetic susceptibility measurements for all complexes demonstrated that antiferromagnetic interactions between the metal ions were in operation. The magnetic susceptibility data of the copper and nickel complexes were analyzed using a tetranuclear model based on $\boldsymbol{H} = -2J(\boldsymbol{S}_1\boldsymbol{S}_2+\boldsymbol{S}_2\boldsymbol{S}_3+\boldsymbol{S}_3\boldsymbol{S}_4+\boldsymbol{S}_4\boldsymbol{S}_1)$ to give best-fit parameters of $g = 2.11(1)$, $J = -1.39(3)$ cm^{-1} and $g = 2.19(1)$, $J = -0.44(2)$ cm^{-1}, respectively.

Keywords: asymmetric multidentate ligands; cobalt; copper; grid; magnetism; nickel; self-assembly.

INTRODUCTION

Bistable molecules are attracting great research interest due to their potential applications as nanoscale molecular switches. For example, metal clusters which display spin crossover (SCO) phenomena (spin transitions between high- (HS) and low-spin (LS) states as a result of the application of external stimuli such as temperature, pressure, light, and magnetic or electric field), have drawn much attention due to the ease with which desirable electronic states can be accessed through ligand modification [1]. A second group of compounds that can show controllable changes in their electronic states are the species that display the charge-transfer-induced spin transition (CTIST) phenomena. CTIST usually occurs by the change of Co(II)HS-Fe(III)LS to Co(III)LS-Fe(II)LS and has been observed in cyanide-bridged cobalt-iron complexes such as Prussian-blue analogues, octanuclear cubic molecules, and tetranuclear

*Paper based on a presentation made at the 11th Eurasia Conference on Chemical Sciences, The Dead Sea, Jordan, 6–10 October 2010. Other presentations are published in this issue, pp. 1643–1799.

‡Corresponding author

square complexes [2]. Other possible systems that may display bistability include photo-isomerizable molecules, valence tautomeric complexes, and mixed-valence systems [3].

We focus on multi-bistable molecules because high-order molecular switches are important candidates for applications in the nanosized devices of the future. We reported a two-step SCO complex, $[Fe^{II}_4(\mu\text{-}CN)_4(bpy)_4(tpa)_2](PF_6)_4$ (bpy = 2,2'-bipyridine, tpa = tris(2-pyridylmethyl)amine), which has three metastable spin states of LS-LS, LS-HS, and HS-HS of the tpa coordinated iron ions [4]. In addition, we recently reported the observation of two-step CTIST in a cyanide-bridged $[Co_2Fe_2]$ square molecule, $[Co_2Fe_2(\mu\text{-}CN)_6(tp^*)_2(dtbbpy)_4](PF_6)_2 \cdot 2MeOH$ [5]. Cyanide-bridged square molecules are good candidates for the construction of clusters that may show multi-bistability. Of course, this potential for constructing functional molecules extends beyond cyanide-bridged systems and our current research concerns the investigation of grid-type molecules as potential switching materials due to their stability, ease of modification, and strength of interactions between metal centers [6]. Grid-type complexes are usually synthesized using rigid and planar multidentate ligands, and amide and polypyridine type ligands have been used to synthesize [$n \times n$] type (n = 2–5) grid complexes [7–9]. Grid molecules of $[Fe_4]$ motifs can show multi-step SCO phenomena due to the provision of N_6 coordination spheres for the iron sites [9a,10]. In line with these findings, we are investigating the development of useful multinucleating ligands suitable for constructing grid-type molecules, and the use of rigid, planar multidentate ligands led to the synthesis of two kinds of tetranuclear manganese complex; $[Mn^{III}_4(L1)_4(\mu_2\text{-}OMe)_4] \cdot 2.5H_2O$ (H_2L1 = 2-[3-(2-hydroxyphenyl)-1*H*-pyrazole-5-yl]-6-pyridinecarboxylic acid methyl ester) and $[Mn^{II}_2Mn^{III}_2(L2)_4(H_2O)_2](PF_6)_2 \cdot CHCl_3 \cdot CH_3OH \cdot 1.5H_2O$ (H_2L2 = 2-[3-(2-hydroxyphenyl)-1*H*-pyrazol-5-yl]-6-pyridinecarboxylic acid ethyl ester), which showed aniferromagnetic interactions and ferromagnetic interactions between metal centers, respectively [11]. Additionally, our recent work led us to find a grid-type single-molecule magnet, $[Co^{II}_8Co^{III}(L)_6]$ (L = 2,6-bis[3-(2-pyridine)-1,3-dioxopropyl]pyridine) [12]. In order to exploit a greater variety of grids, we are using asymmetric multidentate ligands in their syntheses (Scheme 1). This is an important area of research from the viewpoint of extending our knowledge and experience in molecular grids, and may have important applications toward nanoscale functional materials. Herein we report our studies into the rational control of metal ion arrangements in grid-type clusters using asymmetric ligands and present three [2 × 2] grid-type complexes with different metal ions and discuss their magnetic properties.

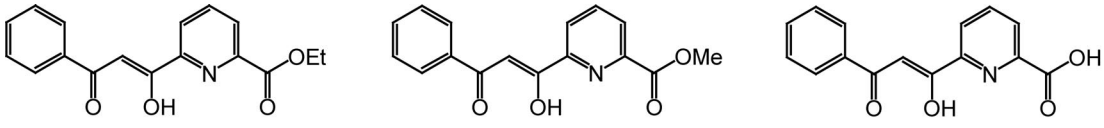

Scheme 1 Multidentate ligands used in this work. Left: 6-[1,3-dioxo-3-(2-phenyl)propionyl]pyridine-2-carboxylic acid ethyl ester (HL). Middle: 6-[1,3-dioxo-3-(2-phenyl)propionyl]pyridine-2-carboxylic acid methyl ester (HL1). Right: 6-[1,3-dioxo-3-(2-phenyl)propionyl]pyridine-2-carboxylic acid (H_2L2).

EXPERIMENTAL METHODS

Materials and physical measurements

All experiments were carried out under ambient conditions. All reagents for the syntheses were commercially available and used without further purification. Elemental analyses were performed using a Perkin Elmer 2400 element analyzer. The FT-IR spectra were obtained with Shimadzu FTIR-8400 infrared spectrometer. Diffraction data of compounds **1**, **2**, and **3** were obtained using a Bruker SMART APEX diffractometer. The structures were solved using direct methods and expanded using the Fourier

technique. All non-hydrogen atoms were refined with anisotropic thermal parameters. Hydrogen atoms were fixed at calculated positions and refined using a riding model. Magnetic data were measured with a MPMS XL5 SQUID susceptometer (Quantum Design). Magnetic susceptibilities were measured in a 1.8–300 K temperature range under an applied magnetic field of 0.05 T. Magnetization at 1.8 K was measured from 0 to 5 T.

Synthesis of 6-[1,3-dioxo-3-(2-phenyl)propionyl]pyridine-2-carboxylic acid ethyl ester (HL)

Sodium ethoxide was prepared from sodium (6.99 g, 304 mmol) in ethanol, and evaporated to dryness to give a white solid which was combined with acetophenone (13.5 g, 112 mmol) and 2,6-pyridine dicarboxylic acid ethyl ester (25.0 g, 112 mmol) in 100 ml of diethyl ether and refluxed for 1 h under nitrogen. The solvent was removed by filtration, and aqueous acetic acid (15 %) was added to the residue. The resulting yellow solid was filtered, and recrystallization of the crude product from ethanol yielded yellow crystals (19.0 g). Yield: 60 %. Anal. calcd. for $C_{17}H_{15}NO_4$: C, 68.68; H, 5.09; N, 4.71 %. Found: C, 68.62; H, 5.25; N, 4.63 %. ^{1}H NMR (270 MHz, DMSO) δ/ppm: 8.26–8.21 (m, 3H, py), 7.70–7.55 (m, 5H, ph), 4.42 (q, J = 7.0 Hz, 2H, CH_2), 1.39 (t, J = 7.0 Hz, 3H, CH_3).

Synthesis of $[Cu_4(L1)_4(NO_3)_4]$ Et_2O 2MeOH (1 Et_2O 2MeOH) (HL1 = 6-[1,3-dioxo-3-(2-phenyl)propionyl]pyridine-2-carboxylic acid methyl ester)

To a solution of $Cu(NO_3)_2{\cdot}3H_2O$ (121 mg, 0.5 mmol) in methanol (8 mL) a mixture of HL (74 mg, 0.25 mmol) and triethylamine (70 μL, 0.5 mmol) in methanol (4 mL) was added. The resulting green solution was filtered and layered with diethylether to give green needle crystals of $[Cu_4(L1)_4(NO_3)_4]{\cdot}Et_2O{\cdot}2MeOH$ (**1**·Et_2O·2MeOH) (HL1 = 6-[1,3-dioxo-3-(2-phenyl)propionyl]pyridine-2-carboxylic acid methyl ester). The crystals were collected by suction and air-dried. Anal. calcd. for $C_{64}H_{48}N_8O_{28}Cu_4$ (**1**): C, 47.32; H, 3.19; N, 6.74 %. Found: C, 47.12; H, 2.97; N, 6.87 %.

Synthesis of $[Ni_4(L2)_4(H_2O)_4]$ 4MeOH 6H_2O (2 4MeOH 6H_2O) (H_2L2 = 6-[1,3-dioxo-3-(2-phenyl)propionyl]pyridine-2-carboxylic acid)

To a solution of $Ni(AcO)_2{\cdot}4H_2O$ (125 mg, 0.5 mmol) in methanol (8 mL) a mixture of HL (74 mg, 0.25 mmol) and triethylamine (70 μL, 0.5 mmol) in methanol (4 mL) was added. The resulting light green solution was filtered and allowed to stand for a few days to give light green prism crystals of $[Ni_4(L2)_4(H_2O)_4]{\cdot}4MeOH{\cdot}6H_2O$ (**2**·4MeOH·6H_2O) (H_2L2 = 6-[1,3-dioxo-3-(2-phenyl)propionyl]pyridine-2-carboxylic acid). The crystals were collected by suction and air-dried. Anal. calcd. for $C_{60}H_{62}N_4Ni_4O_{29}$ (**2**·9H_2O): C, 48.99; H, 3.86; N, 3.75 %. Found: C, 49.16; H, 3.71; N, 3.82 %.

Synthesis of $[Co_4(L2)_4(H_2O)_4]$ 4MeOH 6H_2O (3 4MeOH 6H_2O)

Compound **3** was obtained by the same synthetic approach adopted for compound **2** using $Co(AcO)_2{\cdot}4H_2O$ (125 mg, 0.5 mmol) instead of $Ni(AcO)_2{\cdot}4H_2O$. Red prism crystals of $[Co_4(L2)_4(H_2O)_4]{\cdot}4MeOH{\cdot}6H_2O$ (**3**·4MeOH·6H_2O) were obtained. The crystals were collected by suction and air-dried. Anal. calcd. for $C_{60}H_{66}N_4Co_4O_{31}$ (**3**·11H_2O): C, 45.84; H, 3.92; N, 3.28 %. Found: C, 45.76; H, 4.22; N, 3.56 %.

X-ray crystallography

A green needle crystal of **1** (0.28 × 0.24 × 0.06 mm^3), a light green prism of **2** (0.29 × 0.20 × 0.08 mm^3), and a red prism of **3** (0.40 × 0.20 × 0.19 mm^3) were mounted individually with epoxy resin on

the tip of a glass fiber. Diffraction data were collected at –73 °C on a Bruker SMART APEX diffractometer fitted with a CCD type area detector, and a full sphere of data was collected using graphite-monochromated Mo–Kα radiation ($\lambda = 0.71073$ Å). After data collection, the first 50 frames were recollected to establish that the crystal had not deteriorated during the data collection. The data frames were integrated using SAINT and were merged to give a unique data set for structure determination. Total reflections collected were 23 835, 11 617, and 22 342 for **1**, **2**, and **3**, respectively, of which 16 526 (R(int) = 0.0251), 3649 (R(int) = 0.0595), and 3957 (R(int) = 0.2677) were independent reflections. The structures were solved using direct methods and refined by the full-matrix least-squares method on all F^2 data using the SHELXTL 5.1 package (Bruker Analytical X-ray Systems). Non-hydrogen atoms were refined with anisotropic thermal parameters. Hydrogen atoms were added in their calculated positions and refined with isotropic thermal parameters riding on those of the parent atoms.

The crystallographic data sets for **1**, **2**, and **3** have been deposited to the Cambridge Crystallographic Data Centre with publication citation and deposition numbers CCDC 802665–802667 (**1–3**). Copies of the data can be obtained free of charge on application to CCDC, 12 Union Road, Cambridge CB21EZ, UK, fax: (+44) 1223-336-033; E-mail: deposit@ccdc.cam.ac.uk.

RESULTS AND DISCUSSION

Crystal structures

The crystal structures of three grid compounds were determined by single-crystal X-ray diffraction analyses. Crystallographic data and selected bond distances and angles are given in Tables 1 and 2, respectively.

Table 1 Crystallographic data for complexes **1–3**.

Compound	**1**	**2**	**3**
Formula	$C_{70}H_{66}N_8O_{31}Cu_4$	$C_{64}H_{52}N_4O_{30}Ni_4$	$C_{64}H_{52}N_4O_{30}Co_4$
Formula weight	1769.47	1591.94	1592.82
Crystal color	green	light green	red
Crystal habit	needle	prism	prism
Crystal size/mm^3	0.28 × 0.24 × 0.06	0.29 × 0.20 × 0.08	0.40 × 0.20 × 0.19
Crystal system	Triclinic	Orthorhombic	Orthorhombic
Space group	$P\bar{1}$	*F*ddd	*F*ddd
Unit cell dimensions			
a/Å	14.929(3)	19.514(7)	19.725(4)
b/Å	15.212(3)	20.218(7)	19.996(4)
c/Å	19.018(4)	34.789(14)	34.896(8)
α/°	83.595(4)		
β/°	67.152(3)		
γ/°	86.965(3)		
V/Å^3	3955.0(13)	13 725(8)	13 763(5)
Z	2	8	8
D_{calc}/Mg m^{-3}	1.486	1.541	1.537
Absorption coefficient/mm^{-1}	1.149	1.172	1.038
θ range/°	1.35 to 27.50	1.56 to 27.49	1.56 to 27.50
Reflections collected	23 835	11 617	22 342
Independent reflections (R_{int})	16 526 (0.0251)	3649 (0.0595)	3957 (0.2677)
Final R indices [$I > 2\sigma(I)$]	$R1$ = 0.0592	$R1$ = 0.0428	$R1$ = 0.0635
	$wR2$ = 0.1775	$wR2$ = 0.1098	$wR2$ = 0.0933
Goodness-of fit on F^2	1.000	1.000	0.999

Table 2 Selected bond distances (Å) and angles (°) for complexes **1–3**.

$[Cu_4(L1)_4(NO_3)_4(H_2O)_4]$ (**1**)			
Cu1 O13	1.903(3)	Cu1 O14	1.973(3)
Cu1 O17	1.989(3)	Cu1 N1	2.009(4)
Cu1 O2	2.429(3)	Cu1 O3	2.439(4)
Cu2 O1	1.915(3)	Cu2 O2	1.963(3)
Cu2 O20	1.984(3)	Cu2 N2	2.008(4)
Cu2 O6	2.413(3)	Cu2 O7	2.457(4)
Cu3 O5	1.903(3)	Cu3 O6	1.960(3)
Cu3 O23	2.012(4)	Cu3 N3	2.023(4)
Cu3 O10	2.396(3)	Cu3 O11	2.416(4)
Cu4 O9	1.909(3)	Cu4 O10	1.972(3)
Cu4 O26	2.010(4)	Cu4 N4	2.029(4)
Cu4 O15	2.404(3)	Cu4 O14	2.424(3)
Cu1 O2 Cu2	122.24(14)	Cu2 O6 Cu3	124.55(14)
Cu3 O10 Cu4	124.17(14)	Cu4 O14 Cu1	122.57(14)
$[Ni_4(L2)_4(H_2O)_4]\cdot 4MeOH\cdot 6H_2O$ (**2**)			
Ni1 O1	1.991(2)	Ni1 O2	2.065(2)
Ni1 O5	2.103(2)	Ni2 N1	1.975(2)
Ni2 O3	2.094(2)	Ni2 O2	2.204(2)
Ni1 O2 Ni2	126.40(9)		
$[Co_4(L2)_4(H_2O)_4]\cdot 4MeOH\cdot 6H_2O$ (**3**)			
Co1 O1	1.996(4)	Co1 O2	2.108(4)
Co1 O5	2.152(4)	Co2 N1	1.989(5)
Co2 O3	2.151(4)	Co2 O2	2.172(4)
Co1 O2 Co2	123.16(18)		

The ORTEP diagram of the cluster core of $[Cu_4(L1)_4(NO_3)_4]\cdot Et_2O\cdot 2MeOH$ (**1**$\cdot Et_2O\cdot 2MeOH$) is shown in Fig. 1 (left). Compound **1** crystallizes in the triclinic space group $P\bar{1}$ where the asymmetric unit is one $[Cu_4(L1)_4(NO_3)_4]$ molecule, one diethylether molecule, and two methanol molecules. In **1**, the HL ligand used as a starting material is solvolyzed by methanol and converted to the HL1 ligand with a methyl ester group. This tetranuclear copper complex has a high pseudo-symmetry of S_4 with respect to the special positions of the ligands and copper ions, and has a pseudo $\bar{4}$ rotoinversion axis passing through the middle of the Cu1-Cu3 and Cu3-Cu4 vectors. All copper ions have octahedral coordination environments coordinated by a N_1O_2 donor set of one HL1 ligand, an O_2 donor set of a second HL1 ligand, and one oxygen atom of a monodentate nitrate anion. The copper ions have axially elongated coordination geometries with the Jahn–Teller elongation axes directed toward the oxygen atoms (O2, O3 for Cu1; O6, O7 for Cu2; O10, O11 for Cu3; O14, O15 for Cu4) of the tridentate sites of the ligands. The average bond length of the axial coordination bonds is 2.422(4) Å, while that of the equatorial coordination bonds is 1.973(4) Å. The copper ions are bridged by the oxygen atoms of the β-diketone sites of the ligands with an average Cu-O-Cu angle of 123.4(2)°. The four copper ions are not located on the same plane with an average deviation of each copper ion from the least-squares plane defined by the four copper atoms of 0.3693(3) Å. The average intermetallic separation of two copper ions on one side of the square is 3.864(1) Å, while that between the copper ions located on opposite corners is 5.364(1) Å.

Complex **2** has a similar tetranuclear [2 × 2] grid core structure to **1**, however, there are some substantial differences between the structures of **1** and **2** (Fig. 1, right). Firstly, in the formation of compound **2**, the HL ligands are hydrolyzed and converted to H_2L2, which contains an additional car-

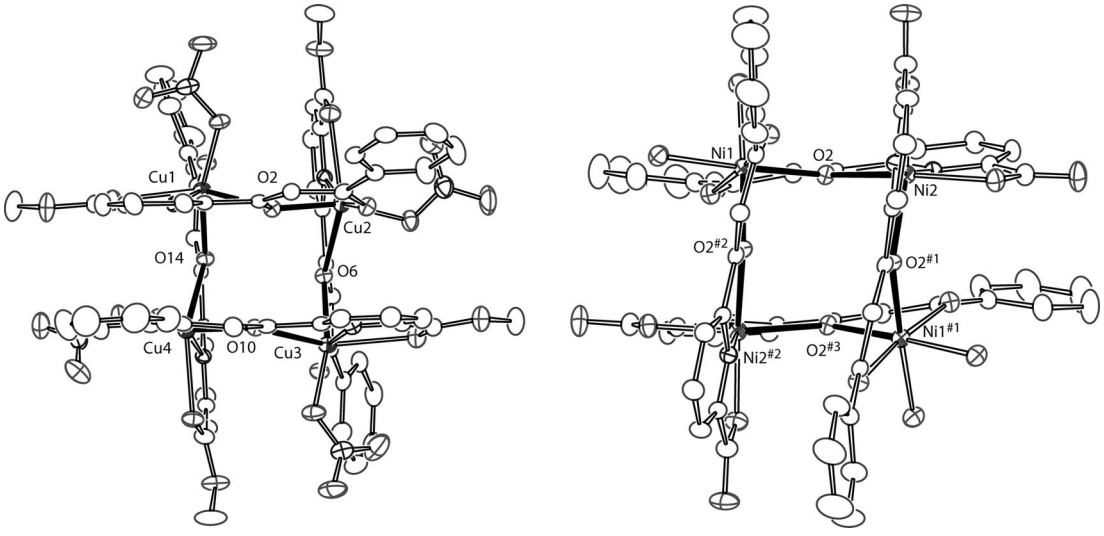

Fig. 1 ORTEP drawing of **1** (left) and **2** (right). Solvent molecules were omitted for clarity. Symmetry operation: #1 +x, 1/4-y, 1/4-z; #2 5/4-x, +y, 1/4-z, #3 5/4-x, 1/4-y, +z.

boxylate group. Compound **2** crystallizes in the orthorhombic space group *F*ddd, where the asymmetric unit contains a quarter of the $[Ni_4(L2)_4(H_2O)_4]$ core, one MeOH, and one and a half H_2O molecules. There are two crystallographically independent nickel ions, located at the tridentate and bidentate sites of ligand and have half occupancy. Each opposite corner pair of nickel ions is located on a two-fold rotation axis, with one parallel to the crystallographic *a* axis and the other to the *b* axis. Thus, the two-fold axes intersect at a right angle at the center of the [2 × 2] grid molecule. Each nickel ion has an octahedral coordination geometry, but the two metal centers have contrasting coordination environments. The Ni1 ions have O_6 donor sets consisting of four oxygen atoms from the β-diketone sites of two L2 ligands and two water molecules. In contrast, the Ni2 ions have N_2O_4 donor sets comprising four oxygen atoms and two nitrogen atoms from the tridentate diacyl pyridine binding sites of the L2 ligands. As a whole, the nickel complex **2** has a relatively low symmetry structure compared with complex **1**. The average bond length of the coordinating bonds is 2.072(2) Å. The nickel ions are bridged by the oxygen atoms of the β-diketone sites of the ligands, with Ni-O-Ni bond angles of 126.40(9)º. All four nickel ions are located on the same plane in complex **2** and the axial coordination bonds of the nickel ions, perpendicular to the plane defined by the four metal centers, are compressed with bond lengths in the range of 1.975(2)–1.991(2) Å, while those along the equatorial plane are in the range of 2.065(2)–2.204(2) Å.

Complex **3** is isostructural to **2**. In the same manner as **2**, the Co1 ions of complex **3** have O6 donor sets consisting of four oxygen atoms from the β-diketone sites of two L2 ligands and two water molecules. The Co2 ions have N_2O_4 donor sets consisting of four oxygen atoms and two nitrogen atoms, from the tridentate diacyl pyridine sites of the L2 ligands. The average bond distance around the metal centers is 2.095(5) Å, and the Co-O-Co bridging angle is 123.16(18)º. In the same manner as complex **2**, four cobalt ions are located on the same plane. In the same manner as **2**, the cobalt coordination bonds that lie perpendicular to the plane defined by the four metal centers are compressed. The bond lengths on the equatorial plane are in the range of 2.108(4)–2.172(4) Å, while those in the axial direction are in the range of 1.989(5)–1.996(4) Å.

Magnetic properties

Magnetic susceptibility measurements were conducted on powder samples of **1**, **2**, and **3** in the temperature range of 1.8–300 K under an external magnetic field of 0.05 Tesla (Fig. 2a). The field dependences of magnetization in **1**, **2**, and **3** were measured in the range of 0–5 T at 1.8 K (Fig. 2b). The magnetic susceptibility data for **1** and **2** were analyzed using the Heisenberg model with one exchange coupling constant J, which is defined by the spin Hamiltonian $\boldsymbol{H} = -2J(\boldsymbol{S}_{M1}\cdot\boldsymbol{S}_{M2}+\boldsymbol{S}_{M2}\cdot\boldsymbol{S}_{M3}+\boldsymbol{S}_{M3}\cdot\boldsymbol{S}_{M4}+\boldsymbol{S}_{M4}\cdot\boldsymbol{S}_{M1})$. The fitting equations can be calculated using Kambe's vector coupling method, supposing identical exchange coupling constants are active in the intra-square magnetic pathways.

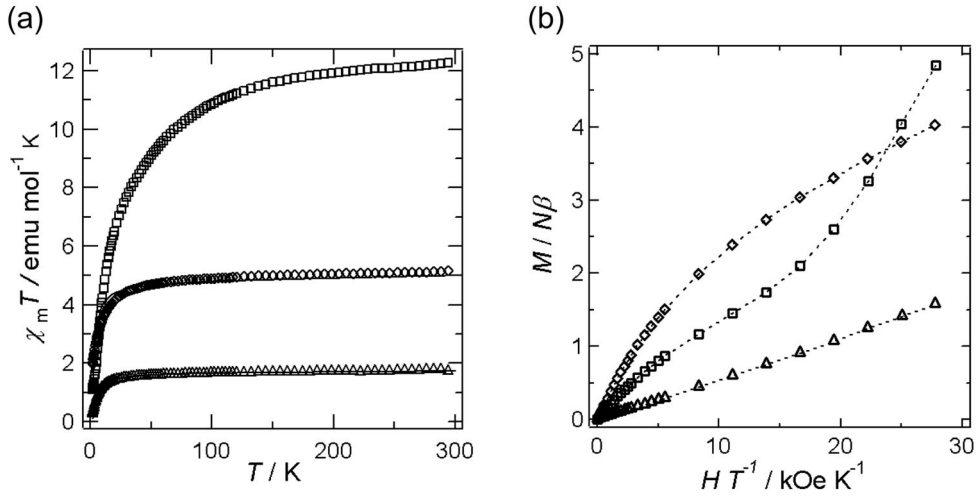

Fig. 2 (a) Plots of $\chi_m T$ vs. T for **1** (□), **2** (○), and **3** (△). Solid line corresponding to the data fitting using the parameters described in the text. (b) Plots of M vs. H for **1** (□), **2** (○), and **3** (△).

*[$Cu_4(L1)_4(NO_3)_4$] (**1**)*

At room temperature, the $\chi_m T$ value was 1.68 emu mol^{-1} K, which is larger than that expected for four uncorrelated S = 1/2 spins (1.50 emu mol^{-1} K, g = 2.00). Upon cooling, the $\chi_m T$ values decreased monotonically to a value of 0.29 emu mol^{-1} K at 1.8 K. This magnetic behavior is indicative of intramolecular antiferromagnetic interactions. The least-squares calculation yielded the best-fit parameters where g and J values were 2.11(1) and –1.39(3) cm^{-1}, respectively. Considering the coordination environments of four copper ions and the bridging fashion of the ligands, it may have been expected that ferromagnetic interactions would be dominant between copper ions due to the orthogonal arrangements of the interacting magnetic orbitals. However, as the bridging angles of the ligands deviate from a straight line, antiferromagnetic interactions may have been encouraged.

*[$Ni_4(L2)_4(H_2O)_4$] 9H_2O (**2** 9H_2O)*

The $\chi_m T$ value at 300 K is 4.67 emu mol^{-1} K, which is slightly larger than the expected values for four magnetically isolated Ni(II) ions (4.00 emu mol^{-1} K, g = 2.00). The $\chi_m T$ values decreased to 1.77 emu mol^{-1} K at 1.8 K upon cooling, suggesting the occurrence of antiferromagnetic interactions between the Ni(II) centers. The least-squares calculation yielded best-fit g and J parameters of 2.19(1) and –0.44(2) cm^{-1}, respectively.

*$[Co_4(L2)_4(H_2O)_4]$ $11H_2O$ (**3** $11H_2O$)*

The $\chi_m T$ value of 10.79 emu mol^{-1} K at 300 K gradually decreased as the temperature was lowered, reaching 0.96 emu mol^{-1} K at 1.8 K. As Co(II) ions have a spin-orbital coupling contribution, the $\chi_m T$ value at room temperature is much larger than the spin-only value for four uncorrelated Co(II) ions, which is expected to be 7.50 emu mol^{-1} K (g = 2.0). The gradual decrease of the $\chi_m T$ value may be due to a combination of spin orbital coupling and antiferromagnetic interactions between cobalt ions. In this complex, the field dependence of magnetization measurements, which showed a distinct magnetization increase in magnetization gradient at higher field, indicate the existence of antiferromagnetic interactions at lower field followed by subsequent spin flip toward ferromagnetic interactions, as the field strength was increased. O. Waldmann et al. reported that a similar grid-type cobalt tetranuclear complex showed metamagnetic-like behavior in magnetization measurements at 1.9 K [6b,c]. In this paper, magnetic measurements conducted on a single crystal indicated that the [2 × 2] grid-type cobalt complex shows an antiferromagnetic spin arrangement at low field strength and has Ising-type interactions between neighboring cobalt ions. The presented results of complex **3** can be considered to show similar behavior to the literature example due to the strong structural resemblance.

CONCLUSION

Three kinds of [2 × 2] grid-type complex were synthesized by the reaction of different metal sources with an asymmetric polynucleating ligand HL in the presence of triethyl amine. All [2 × 2] grid-type complexes were composed of four asymmetric ligands and four metal ions, however, there were significant differences in their coordination styles. These structures can be categorized into two types, the first being the tetranuclear copper complex, where all copper ions have equivalent N_2O_4 coordination environments, with the nickel and cobalt clusters falling into a second group. In these complexes, there are two different kinds of metal ions, one with O_6 donor sets and the other in a N_2O_4 coordination environment. These results suggest that an asymmetric, rigid ligand with different coordination sites can provide self-organized coordination environments dependent upon the kind of metal ions. Cryomagnetic studies revealed that all three compounds show antiferromagnetic interactions between paramagnetic centers. It should be noted that the rare metamagnetic-like behavior in the tetranuclear cobalt grid complex was brought about by a combination of weak antiferromagnetic interactions, and the orientation of the Co(II) single ion anisotropy axes being aligned such as to show Ising-type magnetic anisotropy.

SUPPLEMENTARY INFORMATION

CCDC 802665–802667 contain the supplementary crystallographic data for this paper. These data can be obtained free of charge via <http://www.ccdc.cam.ac.uk/conts/retrieving.html>, or from the Cambridge Crystallographic Data Centre, 12 Union Road, Cambridge CB2 1EZ, UK; fax: (+44) 1223-336-033; or E-mail: deposit@ccdc.cam.ac.uk.

ACKNOWLEDGMENT

This work was supported by a Grant-in-Aid for Scientific Research from the Ministry of Education, Culture, Sports, Science and Technology, Japan.

REFERENCES

1. (a) P. Gütlich, A. Hauser, H. Spiering. *Angew. Chem., Int. Ed. Engl.* **33**, 2024 (1994); (b) J. A. Real, A. B. Gasper, V. Niel, M. C. Munoz. *Coord. Chem. Rev.* **236**, 121 (2003); (c) P. Gütlich, H. A. Goodwin. *Spin Crossover in Transition Metal Compounds I-III*, Springer, New York (2004); (d) O. Kahn, C. J. Martinez. *Science* **279**, 44 (1998); (d) P. Gamez, J. S. Costa, M. Quesada, G. Aromí. *Dalton Trans.* 7845 (2009).
2. CTIST phenomena: (a) O. Sato, T. Iyoda, A. Fujishima, K. Hashimoto. *Science* **272**, 704 (1996); (b) D. Li, R. Clérac, O. Roubeau, E. Harté, C. Mathoniére, R. L. Bris, S. M. Holmes. *J. Am. Chem. Soc.* **130**, 252 (2008); (c) M. G. Hilfiger, M. Chem, T. V. Brinzari, T. M. Nocera, M. Shatruk, D. T. Patasis, J. L. Musfeldt, C. Achim, K. R. Dunbar. *Angew. Chem., Int. Ed.* **49**, 1410 (2010); (d) Y. Zhang, D. Li, R. Clérac, M. Kalisz, C. Mathoniére, S. M. Holmes. *Angew. Chem., Int. Ed.* **49**, 3752 (2010).
3. Bistable molecule: (a) M. Irie. *Chem. Rev.* **100**, 1685 (2000); (b) O. Sato. *Acc. Chem. Res.* **36**, 692 (2003); (c) B. L. Feringa. *Acc. Chem. Res.* **34**, 504 (2001); (c) O. Sato, J. Tao, Y.-Z. Zhang. *Angew. Chem., Int. Ed.* **46**, 2152 (2007); (d) O. Sato, A. Cui, R. Matsuda, J. Tao, S. Hayami. *Acc. Chem. Res.* **40** 361 (2007); (e) K. D. Demadis, C. M. Hartshorn, T. J. Meyer. *Chem. Rev.* **101**, 2655 (2001); (f) W. Kaim, B. Sarkar. *Coord. Chem. Rev.* **251**, 584 (2007).
4. M. Nihei, M. Ui, M. Yokota, L. Han, A. Maeda, H. Kishida, H. Okamoto, H. Oshio. *Angew. Chem., Int. Ed.* **44**, 6484 (2005).
5. (a) M. Nihei, Y. Sekine, N. Suganami, H. Oshio. *Chem. Lett.* **39**, 978 (2010); (b) M. Nihei, Y. Sekine, N. Suganami, K. Nakazawa, A. Nakao, H. Nakao, Y. Murakami, H. Oshio. *J. Am. Chem. Soc.* **133**, 3592 (2011).
6. (a) A. Petitjean, N. Kyritsakas, J. M. Lehn. *Chem. Commun.* 1168 (2004); (b) O. Waldmann, M. Ruben, U. Ziener, P. Müller, J. M. Lehn. *Inorg. Chem.* **45**, 6535 (2006); (c) O. Waldmann, J. Hassmann, P. Müller, G. S. Hanan, D. Volkmer, U. S. Schubert, J.-M. Lehn. *Phys. Rev. Lett.* **78**, 3390 (1997).
7. (a) L. N. Dawe, K. V. Shuvaev, L. K. Thompson. *Chem. Soc. Rev.* **38**, 2334 (2009); (b) L. N. Dawe, K. V. Shuvaev, L. K. Thompson. *Inorg. Chem.* **48**, 3323 (2009).
8. (a) A. R. Stefankiewicz, J.-M. Lehn. *Chem.—Eur. J.* **15**, 2500 (2009); (b) L. H. Uppadine, J.-P. Gisselbrecht, N. Kyritsakas, K. Nättinen, K. Rissanen, J.-M. Lehn. *Chem.—Eur. J.* **11**, 2549 (2005).
9. (a) B. Schneider, S. Demeshko, S. Dechert, F. Meyer. *Angew. Chem., Int. Ed.* **49**, 9274 (2010); (b) J. I. van der Vlugt, S. Demeshko, S. Dechert, F. Meyer. *Inorg. Chem.* **47**, 1576 (2008).
10. D.-Y. Wu, O. Sato, Y. Einaga, C.-Y. Duan. *Angew. Chem., Int. Ed.* **48**, 1475 (2009).
11. T. Matsumoto, T. Shiga, M. Noguchi, T. Onuki, G. N. Newton, N. Hoshino, M. Nakano, H. Oshio. *Inorg. Chem.* **49**, 368 (2010).
12. T. Shiga, T. Matsumoto, M. Noguchi, T. Onuki, N. Hoshino, G. N. Newton, M. Nakano, H. Oshio. *Chem. Asian J.* **4**, 1660 (2009).

